SIAM J. Numer. Anal.
Vol. 54, No. 2, pp. 825–847

ANALYSIS OF MIXED INTERIOR PENALTY DISCONTINUOUS GALERKIN METHODS FOR THE CAHN–HILLIARD EQUATION AND THE HELE–SHAW FLOW*

XIAOBING FENG†, YUKUN LI‡, AND YULONG XING§

Abstract. This paper proposes and analyzes two fully discrete mixed interior penalty discontinuous Galerkin (DG) methods for the fourth order nonlinear Cahn–Hilliard equation. Both methods use the backward Euler method for time discretization and interior penalty DG methods for spatial discretization. They differ from each other on how the nonlinear term is treated; one of them is based on fully implicit time-stepping and the other uses energy-splitting time-stepping. The primary goal of the paper is to prove the convergence of the numerical interfaces of the DG methods to the interface of the Hele–Shaw flow. This is achieved by establishing error estimates that depend on ϵ^{-1} only in some low polynomial orders, instead of exponential orders. Similar to [X. Feng and A. Prohl, *Numer. Math.*, 74 (2004), pp. 47–84], the crux is to prove a discrete spectrum estimate in the discontinuous Galerkin finite element space. However, the validity of such a result is not obvious because the DG space is not a subspace of the (energy) space $H^1(\Omega)$ and it is larger than the finite element space. This difficulty is overcome by a delicate perturbation argument which relies on the discrete spectrum estimate in the finite element space proved by Feng and Prohl. Numerical experiment results are also presented to gauge the theoretical results and the performance of the proposed fully discrete mixed DG methods.

Key words. Cahn–Hilliard equation, Hele–Shaw problem, phase transition, discontinuous Galerkin method, discrete spectral estimate, convergence of numerical interface

AMS subject classifications. 65N12, 65N15, 65N30

DOI. 10.1137/15M1009962

1. Introduction.

This paper concerns mixed interior penalty discontinuous Galerkin (MIP-DG) approximations of the following Cahn–Hilliard problem:

$$u_t - \Delta w = 0 \quad \text{in } \Omega_T := \Omega \times (0,T), \tag{1.1}$$

$$-\epsilon\Delta u + \frac{1}{\epsilon} f(u) = w \quad \text{in } \Omega_T, \tag{1.2}$$

$$\frac{\partial u}{\partial n} = \frac{\partial w}{\partial n} = 0 \quad \text{on } \partial\Omega_T := \partial\Omega \times (0,T), \tag{1.3}$$

$$u = u_0 \quad \text{in } \Omega \times \{t=0\}. \tag{1.4}$$

Here $\Omega \subseteq \mathbf{R}^d$ $(d = 2,3)$ is a bounded domain, and $f(u) = F'(u)$, $F(u)$ is a nonconvex potential density function which takes its global minimum zero at $u = \pm 1$. In this

*Received by the editors February 24, 2015; accepted for publication (in revised form) February 5, 2016; published electronically March 24, 2016. The work of the first and second authors was partially supported by NSF grants DMS-1016173 and DMS-1318486.
http://www.siam.org/journals/sinum/54-2/M100996.html
†Department of Mathematics, University of Tennessee, Knoxville, TN 37996 (xfeng@math.utk.edu).
‡Department of Mathematics, University of Tennessee, Knoxville, TN 37996, and Department of Mathematics, Penn State University, State College, PA 16801 (yfl5134@psu.edu).
§Department of Mathematics, University of Tennessee, Knoxville, TN 37996; Computer Science and Mathematics Division, Oak Ridge National Laboratory, Oak Ridge, TN 37831; and Department of Mathematics, University of California at Riverside, Riverside, CA 92521 (yulong.xing@ucr.edu).
The work of this author was partially supported by NSF grant DMS-1216454 and by Oak Ridge National Laboratory, managed by UT-Battelle, LLC, for the U.S. Department of Energy under contract De-AC05-00OR22725.

paper, we only consider the following quartic potential density function:

$$F(u) = \frac{1}{4}(u^2 - 1)^2. \tag{1.5}$$

After eliminating the intermediate variable w (called the chemical potential), the above system reduces into a fourth order nonlinear PDE for u, which is known as the Cahn–Hilliard equation in the literature. This equation was introduced by John W. Cahn and John E. Hilliard in [5] to describe the process of phase separation, by which the two components of a binary fluid spontaneously separate and form domains pure in each component. Here u and $1 - u$ denote respectively the concentrations of the two fluids, with $u = \pm 1$ indicating domains of the two components. We note that (1.1)–(1.2) differ from the original Cahn–Hilliard equation in the scaling of the time, and t here corresponds to t/ϵ in the original formulation; ϵ, which is positively small, is called the interaction length.

Besides its important role in materials phase transition, the Cahn–Hilliard equation has been extensively studied due to its close relation with the Hele–Shaw problem. It was first formally proved by Pego [19] that the chemical potential $w := -\epsilon\Delta u + \frac{1}{\epsilon}f(u)$ along with the zero-level set of u tends to (as $\epsilon \to 0$) a limit which satisfies a free boundary problem known as the Hele–Shaw problem. A rigorous justification was given by Stoth [22] for the radially symmetric case and by Alikakos, Bates, and Chen [2] for the general case. In addition, Chen [7] established the convergence of the weak solution of the Cahn–Hilliard problem to a weak (or varifold) solution of the Hele–Shaw problem. Moreover, the Cahn–Hilliard equation (together with the Allen–Cahn equation) has become a fundamental equation as well as a building block in the phase field methodology (or the diffuse interface methodology) for moving interface and free boundary problems arising from various applications such as fluid dynamics, materials science, image processing, and biology (cf. [20, 12] and the references therein). The diffuse interface approach provides a convenient mathematical formalism for numerically approximating the moving interface problems because explicitly tracking the interface is not needed in the diffuse interface formulation. The main advantage of the diffuse interface method is its ability to handle with ease singularities of the interfaces. Like many singular perturbation problems, the main computational issue is to resolve the (small) scale introduced by the parameter ϵ in the equation. Computationally, the problem could become intractable, especially in three-dimensional cases if uniform meshes are used. This difficulty is often overcome by exploiting the predictable (at least for small ϵ) PDE solution profile and by using adaptive mesh techniques (cf. [17] and the references therein), so fine meshes are only used in the diffuse interface region.

Numerical approximations of the Cahn–Hilliard equation have been extensively carried out in the past 30 years (cf. [9, 11, 15] and the references therein). On the other hand, the majority of these works were done for a fixed parameter ϵ. The error bounds, which are obtained using the standard Gronwall inequality technique, show an exponential dependence on $1/\epsilon$. Such an estimate is clearly not useful for small ϵ, in particular, in addressing the issue whether the computed numerical interfaces converge to the original sharp interface of the Hele–Shaw problem. Better and practical error bounds should only depend on $1/\epsilon$ in some (low) polynomial orders because they can be used to provide an answer to the above convergence question, which in fact is the best result (in terms of ϵ) one can expect. The first such polynomial order in $1/\epsilon$ a priori estimate was obtained in [16] for mixed finite element approximations of the Cahn–Hilliard problem (1.1)–(1.5). In addition, polynomial order in $1/\epsilon$ a posteriori error estimates were obtained in [17] for the same mixed finite element methods. One of the key ideas employed in all these works is to use a nonstandard error estimate technique which is based on establishing a discrete spectrum estimate (using its continuous counterpart) for the linearized Cahn–Hilliard operator. An immediate corollary of the polynomial order in $1/\epsilon$ a priori and a posteriori error estimates is the convergence of the numerical interfaces of the underlying mixed finite element approximations to the Hele–Shaw flow before the onset of singularities of the Hele–Shaw flow as ϵ and mesh sizes h and k all tend to zero.

The objective of this paper is twofold. First, we develop some MIP-DG methods to establish polynomial order in $1/\epsilon$ a priori error bounds, as well as to prove convergence of numerical interfaces for the MIP-DG methods. This goal is motivated by the advantages of DG methods in regard to designing adaptive mesh methods and algorithms, which is an indispensable strategy with the diffuse interface methodology. Second, we use the Cahn–Hilliard equation as another prototypical model problem [13] to develop new analysis techniques for analyzing convergence of numerical interfaces to the underlying sharp interface for DG (and nonconforming elements) discretizations of phase field models. To the best of our knowledge, no such convergence result and technique is available in the literature for fourth order PDEs. The main obstacle for improving the finite element techniques of [16] is that the DG (and nonconforming finite element) spaces are not subspaces of $H^1(\Omega)$. As a result, whether the needed discrete spectrum estimate holds becomes a key question to answer.

This paper consists of four additional sections. In section 2, we first introduce function and space notation as well as general assumptions on initial datum u_0; we then cite one important technical lemma which gives a spectral estimate for the linearized Cahn–Hilliard operator. In section 3, we propose two fully discrete MIP-DG schemes for problem (1.1)–(1.5); they differ only in their treatment of the nonlinear term. We then establish a discrete spectrum estimate in the DG space, which mimics the spectral estimates for the differential operator and its finite element counterpart. The main result of this section is to derive optimal error bounds which depend on $1/\epsilon$ only in low polynomial orders for both fully discrete MIP-DG methods. In section 4, using the refined error estimates of section 3, we prove the convergence of the numerical interfaces of the fully discrete MIP-DG methods to the interface of the Hele–Shaw flow before the onset of the singularities as ϵ, h, and k all tend to zero. Finally, in section 5 we provide some numerical experiments to gauge the performance of the proposed fully discrete MIP-DG methods.

This paper is a condensed version of [14], which contains more details that cannot be included here due to the page limitation.

2. Preliminaries. In this section, we shall collect some known results about problem (1.1)–(1.5) from [6, 15, 16], which will be used in sections 3 and 4. Some general assumptions on the initial condition, as well as some energy estimates based on these assumptions, will be cited. Standard function and space notations are adopted in this paper [1, 4]. We use $(\cdot,\cdot)$ and $\|\cdot\|_{L^2}$ to denote the standard inner product and norm on $L^2(\Omega)$. Throughout this paper, C denotes a generic positive constant independent of ϵ, space and time step sizes h and k, which may have different values at different occasions.

We begin with the well-known fact [2] that the Cahn–Hilliard equation (1.1)–(1.5) can be interpreted as the H^{-1}-gradient flow for the Cahn–Hilliard energy functional

$$J_\epsilon(v) := \int_\Omega \Big(\frac{\epsilon}{2}|\nabla v|^2 + \frac{1}{\epsilon}F(v)\Big)\,dx. \tag{2.1}$$

The following *general assumptions* on the initial datum u_0 were made in [15] and were used to derive a priori estimates for the solution of problem (1.1)–(1.5). Suppose that there exists nonnegative constants σ_i for $i = 1, 2, 3, 4$ such that

$$m_0 := \frac{1}{|\Omega|} \int_\Omega u_0(x)dx \in [-1, 1], \tag{2.2}$$

$$J_\epsilon(u_0) \le C\epsilon^{-2\sigma_1}, \tag{2.3}$$

$$\big\| -\epsilon\Delta u_0 + \epsilon^{-1} f(u_0)\big\|_{H^\ell(\Omega)} \le C\epsilon^{-\sigma_{2+\ell}}, \quad \ell = 0, 1, 2. \tag{2.4}$$

Under the above assumptions, some solution estimates were proved, and we refer to [15, 16] for the details.

Next, we quote a lemma which concerns with a lower bound estimate for the principal eigenvalue of the linearized Cahn–Hilliard operator. A proof of this lemma can be found in [6].

LEMMA 2.1. *Suppose that* (2.2)–(2.4) *hold. Given a smooth initial curve/surface* Γ_0*, let* u_0 *be a smooth function satisfying* $\Gamma_0 = \{x \in \Omega; u_0(x) = 0\}$ *and some profile described in* [6]*. Let* u *be the solution to problem* (1.1)–(1.5)*. Define* $\mathcal{L}_{CH}$ *as*

$$\mathcal{L}_{CH} := \Delta\left(\epsilon\Delta - \frac{1}{\epsilon} f'(u)I\right). \tag{2.5}$$

Then there exists $0 < \epsilon_0 << 1$ *and a positive constant* C_0 *such that the principle eigenvalue of the linearized Cahn–Hilliard operator* $\mathcal{L}_{CH}$ *satisfies*

$$\lambda_{CH} := \inf_{\substack{0\ne\psi\in H^1(\Omega)\\ \Delta w=\psi}} \frac{\epsilon\|\nabla\psi\|_{L^2}^2 + \frac{1}{\epsilon}(f'(u)\psi, \psi)}{\|\nabla w\|_{L^2}^2} \ge -C_0 \tag{2.6}$$

for $t \in [0, T]$ *and* $\epsilon \in (0, \epsilon_0)$.

We remark that a discrete generalization of (2.6) on C^0 finite element spaces was proved in [15, 16]. One of main task of this paper is to prove a discrete generalization of (2.6) on the DG space. The restriction on the initial function u_0 is needed to ensure that the solution $u(t)$ satisfies a certain profile for $t > 0$ which is required in the proof of [6]. One such an example is $u_0 = \tanh(\frac{d_0(x)}{\epsilon})$, where $d_0(x)$ stands for the signed distance function to the initial interface Γ_0. Clearly, u_0 is smooth when Γ_0 is smooth.

3. Fully discrete MIP-DG approximations. In this section we present and analyze two fully discrete MIP-DG methods for the Cahn–Hilliard problem (1.1)–(1.5). The primary goal of this section is to derive error estimates for the DG solutions that depend on ϵ^{-1} only in low polynomial orders, instead of exponential orders. As in the finite element case (cf. [16]), the crux is to establish a discrete spectrum estimate for the linearized Cahn–Hilliard operator on the DG space.

3.1. Formulations of the MIP-DG method. Let $\mathcal{T}_h = \{K\}_{K\in\Omega}$ be a quasi-uniform triangulation of Ω parameterized by $h > 0$. For any triangle/tetrahedron $K \in \mathcal{T}_h$, we define h_K to be the diameter of K, and $h := \max_{K\in\mathcal{T}_h} h_K$. The standard broken Sobolev space is defined as

$$H^s(\mathcal{T}_h) := \big\{v \in L^2(\Omega);\, \forall K \in \mathcal{T}_h,\, v|_K \in H^s(K)\big\}. \tag{3.1}$$

For any $K \in \mathcal{T}_h$, $P_r(K)$ denotes the set of all polynomials of degree at most $r(\ge 1)$ on the element K, and the DG finite element space V_h is defined as

$$V_h := \big\{v \in L^2(\Omega);\, \forall K \in \mathcal{T}_h,\, v|_K \in P_r(K)\big\}. \tag{3.2}$$

Let L^2_0 denote the set of functions in $L^2(\Omega)$ with zero mean, and let $\mathring{V}_h := V_h \cap L^2_0$. We also define $\mathcal{E}_h^I$ to be the set of all interior edges/faces of $\mathcal{T}_h$, $\mathcal{E}_h^B$ to be the set of all boundary edges/faces of $\mathcal{T}_h$ on $\Gamma = \partial\Omega$, and $\mathcal{E}_h := \mathcal{E}_h^I \cup \mathcal{E}_h^B$. Let e be an interior edge shared by two elements K_1 and K_2. For a scalar function v, define

$$\{v\} = \frac{1}{2}(v|_K + v|_{K'}), \quad [v] = v|_K - v|_{K'}, \quad \text{on } e \in \mathcal{E}_h^I,$$

where K is K_1 or K_2, whichever has the bigger global labeling, and K' is the other.

Let $0 \le t_0 < t_1 < \cdots < t_M = T$ be a partition of the interval $[0, T]$ with time step $k = t_{n+1} - t_n$. Our fully discrete MIP-DG methods are defined as follows: for any $1 \le m \le M$, $(U^m, W^m) \in V_h \times V_h$ are given by

$$(d_t U^m, \eta) + a_h(W^m, \eta) = 0 \qquad \forall\, \eta \in V_h, \tag{3.3}$$

$$\epsilon a_h(U^m, v) + \frac{1}{\epsilon}(f^m, v) - (W^m, v) = 0 \qquad \forall\, v \in V_h, \tag{3.4}$$

where

$$\begin{aligned} a_h(u, v) = &\sum_{K \in \mathcal{T}_h} \int_K \nabla u \cdot \nabla v \, dx - \sum_{e \in \mathcal{E}_h^I} \int_e \{\nabla u \cdot \mathbf{n}_e\}[v] \, ds \\ &- \sum_{e \in \mathcal{E}_h^I} \int_e \{\nabla v \cdot \mathbf{n}_e\}[u] \, ds + \sum_{e \in \mathcal{E}_h^I} \int_e \frac{\sigma_e^0}{h_e}[u][v] \, ds, \end{aligned} \tag{3.5}$$

$\sigma_e^0 > 0$ is the penalty parameter, and

$$f^m = (U^m)^3 - U^{m-1} \qquad \text{or} \qquad f^m = (U^m)^3 - U^m,$$

which lead to the energy-splitting scheme and fully implicit scheme, respectively. d_t is the (backward) difference operator defined by $d_t U^m := (U^m - U^{m-1})/k$ and $U^0 := \widehat{P}_h u_0$ (or $\widehat{Q}_h u_0$) is the starting value, with the finite element H^1 (or L^2) projection $\widehat{P}_h$ (or $\widehat{Q}_h$) to be defined below. We refer to [13] for the details on why the continuous projection is needed for the initial condition. We remark that only the fully implicit case was considered in [15, 16] for the mixed finite element method.

To analyze the stability of (3.3)–(3.4), we need some preparations. First, we introduce three projection operators that will be needed to derive the error estimates in section 3.4. $P_h : H^s(\mathcal{T}_h) \to V_h$ denotes the elliptic projection operator defined by

$$a_h(u - P_h u, v_h) + (u - P_h u, v_h) = 0 \qquad \forall\, v_h \in V_h, \tag{3.6}$$

which has the following approximation properties (see [8]):

$$\|v - P_h v\|_{L^2(\mathcal{T}_h)} + h\|\nabla(v - P_h v)\|_{L^2(\mathcal{T}_h)} \le Ch^{\min\{r+1,s\}}\|u\|_{H^s(\mathcal{T}_h)}, \tag{3.7}$$

$$\frac{1}{|\ln h|^{\overline{r}}}\|v - P_h v\|_{L^\infty(\mathcal{T}_h)} + h\|\nabla(u - P_h u)\|_{L^\infty(\mathcal{T}_h)} \le Ch^{\min\{r+1,s\}}\|u\|_{W^{s,\infty}(\mathcal{T}_h)}. \tag{3.8}$$

Here $\overline{r} := \min\{1, r\} - \min\{1, r-1\}$.

Let $\widehat{P}_h : H^s(\mathcal{T}_h) \to S_h := V_h \cap C^0(\overline{\Omega})$ denote the standard continuous finite element elliptic projection, which is the counterpart of projection P_h. It has the following well-known property [15, 16]:

$$\|u - \widehat{P}_h u\|_{L^\infty} \le Ch^{2-\frac{d}{2}}\|u\|_{H^2}. \tag{3.9}$$

Next, for any DG function $\Psi_h \in V_h$, we define its continuous finite element projection $\Psi_h^{FE} \in S^h$ by

$$\tilde{a}_h(\Psi_h^{FE}, v_h) = \tilde{a}_h(\Psi_h, v_h) \qquad \forall\, v_h \in S_h, \tag{3.10}$$

where $\tilde{a}_h(u,v) = a_h(u,v) + \alpha(u,v)$, and α is a parameter that will be specified later in section 3.3.

A mesh-dependent H^{-1} norm will also be needed. To this end, we introduce the inverse discrete Laplace operator $\Delta_h^{-1} : \mathring{V}_h \to \mathring{V}_h$ as follows: given $\zeta \in \mathring{V}_h$, let $\Delta_h^{-1}\zeta \in \mathring{V}_h$ such that

$$a_h(-\Delta_h^{-1}\zeta, w_h) = (\zeta, w_h) \qquad \forall\, w_h \in V_h. \tag{3.11}$$

We note that Δ_h^{-1} is well defined provided that $\sigma_e^0 > \sigma_*^0$ for some positive number σ_*^0 and for all $e \in \mathcal{E}_h$ because this condition ensures the coercivity of the DG bilinear form $a_h(\cdot,\cdot)$.

Let $\xi, \zeta \in \mathring{V}_h$; we then define the "–1" inner product by

$$(\zeta,\xi)_{-1,h} := a_h(-\Delta_h^{-1}\zeta, -\Delta_h^{-1}\xi) = (\zeta, -\Delta_h^{-1}\xi) = (-\Delta_h^{-1}\zeta, \xi), \tag{3.12}$$

and the induced mesh-dependent H^{-1} norm is given by

$$\|\zeta\|_{-1,h} := \sqrt{(\zeta,\zeta)_{-1,h}} = \sup_{0\neq\xi\in\mathring{V}_h} \frac{(\zeta,\xi)}{|||\xi|||_a}, \tag{3.13}$$

where $|||\xi|||_a := \sqrt{a_h(\xi,\xi)}$. The following properties can be easily verified (cf. [3]):

$$|(\zeta,\xi)| \le \|\zeta\|_{-1,h}|||\xi|||_a \qquad \forall\, \xi \in V_h,\ \zeta \in \mathring{V}_h, \tag{3.14}$$

$$\|\zeta\|_{-1,h} \le C\|\zeta\|_{L^2} \qquad \forall\, \zeta \in \mathring{V}_h, \tag{3.15}$$

$$\|\zeta\|_{L^2} \le Ch^{-1}\|\zeta\|_{-1,h} \qquad \forall\, \zeta \in \mathring{V}_h. \tag{3.16}$$

3.2. Discrete energy law and well-posedness. In this subsection we first establish a discrete energy law, which mimics the differential energy law, for both fully discrete MIP-DG methods defined in (3.3)–(3.4). Based on this discrete energy law, we then prove the existence and uniqueness of solutions to the MIP-DG methods by recasting the schemes as convex minimization problems at each time step.

THEOREM 3.1. *Let* $(U^m, W^m) \in V_h \times V_h$ *be a solution to scheme* (3.3)–(3.4)*. The following energy law holds for any* $h, k > 0$*:*

$$\begin{aligned} E_h(U^\ell) + k\sum_{m=1}^{\ell}\|d_tU^m\|_{-1,h}^2 + k^2\sum_{m=1}^{\ell}\Big\{\frac{\epsilon}{2}|||d_tU^m|||_a^2 + \frac{1}{4\epsilon}\|d_t(U^m)^2\|_{L^2}^2 \\ + \frac{1}{2\epsilon}\|U^m d_tU^m\|_{L^2}^2 \pm \frac{1}{2\epsilon}\|d_tU^m\|_{L^2}^2\Big\} = E_h(U^0) \end{aligned} \tag{3.17}$$

for all $1 \le \ell \le M$*, where*

$$E_h(U) := \frac{1}{4\epsilon}\|U^2-1\|_{L^2}^2 + \frac{\epsilon}{2}|||U|||_a^2. \tag{3.18}$$

Note that the sign "$\pm$" in (3.17) takes "+" when $f^m = (U^m)^3 - U^{m-1}$ and "−" when $f^m = (U^m)^3 - U^m$.

An immediate consequence of the above discrete energy law is the following stability and well-posedness results.

COROLLARY 3.2. *Let $\sigma_*^0 > 0$ be a sufficiently large constant. Suppose that $\sigma_e^0 > \sigma_*^0$ for all $e \in \mathcal{E}_h$. Then scheme (3.3)–(3.4) is stable for all $h, k > 0$ when $f^m = (U^m)^3 - U^{m-1}$ and is stable for $h > 0$ and $k = O(\epsilon^3)$ when $f^m = (U^m)^3 - U^m$.*

THEOREM 3.3. *Suppose that $\sigma_e^0 > \sigma_*^0$ for all $e \in \mathcal{E}_h$. Then scheme (3.3)–(3.4) has a unique solution (U^m, W^m) at each time step for for all $h, k > 0$ in the case $f^m = (U^m)^3 - U^{m-1}$ and for $h > 0$ and $k = O(\epsilon^3)$ in the case $f^m = (U^m)^3 - U^m$.*

We omit the proofs of the above theorems and corollary to save space and refer the reader to [14] for the details.

3.3. Discrete spectrum estimate on the DG space. In this subsection, we shall establish a discrete spectrum estimate for the linearized Cahn–Hilliard operator on the DG space, which plays a vital role in our error estimates.

PROPOSITION 3.4. *Suppose the assumptions of Lemma 2.1 hold. Let u be the solution of (1.1)–(1.5) and $P_h u$ denote its DG elliptic projection. Assume*

$$\operatorname*{ess\,sup}_{t\in[0,\infty)} \|u\|_{W^{s,\infty}} \le C\epsilon^{-\gamma} \tag{3.19}$$

for a (small) constant γ; then there exists $0 < \epsilon_2 << 1$ and an ϵ-independent and h-independent constant $c_0 > 0$ such that for any $\epsilon \in (0, \epsilon_2)$, there holds

$$\lambda_{CH}^{DG} = \inf_{0\neq\Phi_h\in L_0^2(\Omega)\bigcap V_h} \frac{\epsilon a_h(\Phi_h,\Phi_h) + \frac{1-\epsilon^3}{\epsilon}(f'(P_h u)\Phi_h,\Phi_h)}{\|\nabla\Delta^{-1}\Phi_h\|_{L^2}^2} \ge -c_0, \tag{3.20}$$

provided that h satisfies the constraints

$$h^{2-\frac{d}{2}} \le (C_1C_2)^{-1}\epsilon^{\max\{\sigma_1+\frac{11}{2},\sigma_3+4\}}, \tag{3.21}$$

$$h^{1+r}|\ln h|^{\bar r} \le (C_1C_3)^{-1}\epsilon^{\gamma+3}, \tag{3.22}$$

where C_j for $j = 1, 2, 3$ are defined by

$$C_1 := \max_{|\xi|\le 2C_0} |f''(\xi)|, \tag{3.23}$$

$$\|u - \widehat{P}_h u\|_{L^\infty((0,T);L^\infty)} \le C_2 h^{2-\frac{d}{2}}\epsilon^{\min\{-\sigma_1-\frac{5}{2},-\sigma_3-1\}}, \tag{3.24}$$

$$\|u - P_h u\|_{L^\infty((0,T);L^\infty)} \le C_3 h^{1+r}|\ln h|^{\bar r}\epsilon^{-\gamma}. \tag{3.25}$$

Proof. By Proposition 2 in [15], under the mesh constraint (3.21), we have

$$\|f'(\widehat{P}_h u) - f'(u)\|_{L^\infty((0,T);L^\infty)} \le \epsilon^3. \tag{3.26}$$

Similarly, under condition (3.22), by (3.8), (3.19), and Lemma 2.2 in [16], we can show that for any $\epsilon > 0$, there holds

$$\|f'(P_h u) - f'(u)\|_{L^\infty((0,T);L^\infty)} \le \epsilon^3. \tag{3.27}$$

It follows from (3.26) and (3.27) that

$$\|f'(P_h u) - f'(\widehat{P}_h u)\|_{L^\infty((0,T);L^\infty)} \le 2\epsilon^3 \quad \text{and} \quad f'(P_h u) \ge f'(\widehat{P}_h u) - 2\epsilon^3. \tag{3.28}$$

Therefore,

$$
\begin{aligned}
(3.29)\quad & \epsilon a_h(\Phi_h, \Phi_h) + \frac{1-\epsilon^3}{\epsilon}\big(f'(P_h u)\Phi_h, \Phi_h\big) \\
&\geq \epsilon \frac{1-\epsilon^3}{1-\frac{\epsilon^3}{2}} a_h(\Phi_h, \Phi_h) + \frac{1-\epsilon^3}{\epsilon} \int_\Omega f'(\widehat{P}_h u)\Big((\Phi_h)^2 - (\Phi_h^{FE})^2\Big)\, dx \\
&\quad + \frac{1-\epsilon^3}{\epsilon} \int_\Omega f'(\widehat{P}_h u)(\Phi_h^{FE})^2 dx - 2\epsilon^2(1-\epsilon^3)\|\Phi_h\|_{L^2}^2 + \frac{\epsilon^4}{2-\epsilon^3} a_h(\Phi_h, \Phi_h).
\end{aligned}
$$

Next, we derive a lower bound for each of the first two terms on the right-hand side of (3.29). Notice that the first term can be rewritten as

$$
\begin{aligned}
(3.30)\quad a_h(\Phi_h, \Phi_h) &= a_h(\Phi_h - \Phi_h^{FE}, \Phi_h - \Phi_h^{FE}) + \|\nabla \Phi_h^{FE}\|_{L^2}^2 + 2\alpha\|\Phi_h^{FE} - \Phi_h\|_{L^2}^2 \\
&\quad + 2\alpha\big(\Phi_h^{FE} - \Phi_h, \Phi_h\big).
\end{aligned}
$$

To bound $\|\Phi_h - \Phi_h^{FE}\|_{L^2}$ from above, we consider the following auxiliary problem:

$$
\widetilde{a}_h(\phi, \chi) = \big(\Phi_h - \Phi_h^{FE}, \chi\big) \qquad \forall\, \chi \in H^1(\Omega).
$$

For $\sigma_e^0 > \sigma_*^0$ for all $e \in \mathcal{E}_h$, the above problem has a unique solution $\phi \in H^{1+\theta}(\Omega)$ for $0 < \theta \leq 1$ such that

$$
(3.31)\qquad \|\phi\|_{H^{1+\theta}(\Omega)} \leq C\|\Phi_h - \Phi_h^{FE}\|_{L^2} \qquad \text{for } \theta \in (0, 1].
$$

By the definition of Φ_h^{FE}, we immediately get the following Galerkin orthogonality:

$$
\widetilde{a}_h\big(\Phi_h - \Phi_h^{FE}, \chi_h\big) = 0 \qquad \forall \chi_h \in S_h.
$$

It follows from the duality argument (cf. [21, Theorem 2.14]) that

$$
(3.32)\qquad \|\Phi_h - \Phi_h^{FE}\|_{L^2}^2 \leq Ch^{2\theta} a_h(\Phi_h - \Phi_h^{FE}, \Phi_h - \Phi_h^{FE}) + Ch^{2\theta}\alpha\|\Phi_h - \Phi_h^{FE}\|_{L^2}^2.
$$

For all h satisfying $Ch^{2\theta}\alpha < 1$, we get

$$
(3.33)\qquad \|\Phi_h - \Phi_h^{FE}\|_{L^2}^2 \leq \frac{Ch^{2\theta}}{1 - Ch^{2\theta}\alpha} a_h(\Phi_h - \Phi_h^{FE}, \Phi_h - \Phi_h^{FE}).
$$

Now the last term on the right-hand side of (3.30) can be bounded as follows:

$$
(3.34)\qquad 2\alpha\big(\Phi_h^{FE} - \Phi_h, \Phi_h\big) \geq -\frac{1}{2} a_h(\Phi_h - \Phi_h^{FE}, \Phi_h - \Phi_h^{FE}) - \frac{2C\alpha^2 h^{2\theta}}{1 - Ch^{2\theta}\alpha}\|\Phi_h\|_{L^2}^2.
$$

The second term on the right-hand side of (3.29) can be bounded by

$$
\begin{aligned}
(3.35)\quad & \int_\Omega f'(\widehat{P}_h u)\big((\Phi_h)^2 - (\Phi_h^{FE})^2\big)\, dx \geq -C\int_\Omega \big|(\Phi_h)^2 - (\Phi_h^{FE})^2\big|\, dx \\
&\geq -C\|\Phi_h - \Phi_h^{FE}\|_{L^2}^2 - \frac{\epsilon^3(1-\epsilon^3)}{1-\frac{\epsilon^3}{2}}\|\Phi_h\|_{L^2}^2 - C\frac{1-\frac{\epsilon^3}{2}}{\epsilon^3(1-\epsilon^3)}\|\Phi_h - \Phi_h^{FE}\|_{L^2}^2.
\end{aligned}
$$

Here we have used the facts [16, Lemma 2.2] that

$$
(3.36)\qquad \|u\|_{L^\infty((0,T);L^\infty)} \leq C, \qquad |f'(\widehat{P}_h u)| \leq |f'(u)| + \epsilon^3 \leq C.
$$

Substituting (3.33) into (3.35) yields

$$\begin{aligned}\frac{1-\epsilon^3}{\epsilon}\int_\Omega f'(\widehat{P}_h u)\big((\Phi_h)^2-(\Phi_h^{FE})^2\big)\,dx \\ \geq -\gamma_3\frac{\epsilon(1-\epsilon^3)}{1-\frac{\epsilon^3}{2}}a_h(\Phi_h-\Phi_h^{FE},\Phi_h-\Phi_h^{FE})-\frac{\epsilon^2(1-\epsilon^3)}{1-\frac{\epsilon^3}{2}}\|\Phi_h\|_{L^2}^2,\end{aligned} \tag{3.37}$$

where h is chosen small enough such that $\gamma_3<1/4$.

The term $\|\Phi_h\|_{L^2}^2$ can be bounded by

$$\|\Phi_h\|_{L^2}^2=a_h(\Delta_h^{-1}\Phi_h,\Phi_h)\leq\frac{\rho}{2}a_h(\Delta_h^{-1}\Phi_h,\Delta_h^{-1}\Phi_h)+\frac{1}{2\rho}a_h(\Phi_h,\Phi_h) \tag{3.38}$$

for any constant $\rho>0$. Adding the fifth term on the right-hand side of (3.29), the last term on the right-hand side of (3.34), and that of (3.37), we get for all h satisfying $2C\alpha^2h^{2\theta}/(1-Ch^{2\theta}\alpha)\leq\epsilon$

$$\begin{aligned}-\left(\frac{\epsilon(1-\epsilon^3)}{1-\frac{\epsilon^3}{2}}\,\frac{2C\alpha^2h^{2\theta}}{1-Ch^{2\theta}\alpha}+\frac{3\epsilon^2(1-\epsilon^3)}{1-\frac{\epsilon^3}{2}}\right)\|\Phi_h\|_{L^2}^2\geq-\frac{4\epsilon^2(1-\epsilon^3)}{1-\frac{\epsilon^3}{2}}\|\Phi_h\|_{L^2}^2 \\ \geq-\frac{\epsilon^4}{2(2-\epsilon^3)}a_h(\Phi_h,\Phi_h)-Ca_h(\Delta_h^{-1}\Phi_h,\Delta_h^{-1}\Phi_h).\end{aligned} \tag{3.39}$$

Combining (3.30), (3.34), (3.37), and (3.39) with (3.29), we have

$$\begin{aligned}\epsilon a_h(\Phi_h,\Phi_h)+\frac{1-\epsilon^3}{\epsilon}\int_\Omega f'(P_hu)(\Phi_h)^2\,dx \\ \geq\frac{\epsilon(1-\epsilon^3)}{4-2\epsilon^3}a_h(\Phi_h-\Phi_h^{FE},\Phi_h-\Phi_h^{FE})+\frac{2\alpha\epsilon(1-\epsilon^3)}{1-\frac{\epsilon^3}{2}}\|\Phi_h^{FE}-\Phi_h\|_{L^2}^2 \\ +\frac{\epsilon(1-\epsilon^3)}{1-\frac{\epsilon^3}{2}}\|\nabla\Phi_h^{FE}\|_{L^2}^2-Ca_h(\Delta_h^{-1}\Phi_h,\Delta_h^{-1}\Phi_h) \\ +\frac{1-\epsilon^3}{\epsilon}\int_\Omega f'(\widehat{P}_hu)(\Phi_h^{FE})^2\,dx+\frac{\epsilon^4}{2(2-\epsilon^3)}a_h(\Phi_h,\Phi_h).\end{aligned} \tag{3.40}$$

Applying the finite element spectrum estimate of [14, Lemma 3.4], we get

$$\frac{\epsilon}{1-\frac{\epsilon^3}{2}}\|\nabla\Phi_h^{FE}\|_{L^2}^2+\frac{1}{\epsilon}\int_\Omega f'(\widehat{P}_hu)(\Phi_h^{FE})^2\,dx\geq-\frac{1+C_0}{1-\frac{\epsilon^3}{2}}\|\nabla\Delta^{-1}\Phi_h^{FE}\|_{L^2}^2,$$

which together with (3.40) implies that

$$\begin{aligned}\epsilon a_h(\Phi_h,\Phi_h)+\frac{1-\epsilon^3}{\epsilon}\int_\Omega f'(P_hu)(\Phi_h)^2\,dx \\ \geq-Ca_h(\Delta_h^{-1}\Phi_h,\Delta_h^{-1}\Phi_h)-C\|\nabla\Delta^{-1}\Phi_h^{FE}\|_{L^2}^2+\frac{2\alpha\epsilon(1-\epsilon^3)}{1-\frac{\epsilon^3}{2}}\|\Phi_h^{FE}-\Phi_h\|_{L^2}^2.\end{aligned} \tag{3.41}$$

By the stability of Δ^{-1}, we have

$$\|\nabla\Delta^{-1}(\Phi_h-\Phi_h^{FE})\|_{L^2}^2\leq\widehat{C}\|\Phi_h-\Phi_h^{FE}\|_{L^2}^2,$$

which together with the triangle inequality yields

$$\|\nabla\Delta^{-1}\Phi_h^{FE}\|_{L^2}^2 \le 2\|\nabla\Delta^{-1}\Phi_h\|_{L^2}^2 + 2\widehat{C}\|\Phi_h - \Phi_h^{FE}\|_{L^2}^2.$$

Similarly, since $\Delta_h^{-1}\Phi_h$ is the elliptic projection of $\Delta^{-1}\Phi_h$, there holds

$$a_h(\Delta_h^{-1}\Phi_h, \Delta_h^{-1}\Phi_h) \le C\|\nabla\Delta^{-1}\Phi_h\|_{L^2}^2.$$

Therefore, choosing $\alpha = O(\widehat{C}\epsilon^{-1})$, (3.41) can be further reduced into

$$\epsilon a_h(\Phi_h, \Phi_h) + \frac{1-\epsilon^3}{\epsilon}\int_\Omega f'(P_h u)(\Phi_h)^2\,dx \ge -c_0\|\nabla\Delta^{-1}\Phi_h\|_{L^2}^2$$

for some $c_0 > 0$. This proves (3.20), and the proof is complete. ∎

Remark 3.1. The assumption (3.19) on the solution u is needed to get the (standard) estimate (3.25) for the projection operator P_h. It was also used in [16] to derive the finite element spectrum estimate. The power γ in (3.19) depends on the Sobolev space index s and σ_j for $j = 1, 2, 3, 4$ from (2.2)–(2.4). For the linear finite element, the optimal $s = 2$. In this case, it is easy to check that $\gamma \le \sigma_4$ by using the Sobolev embedding $H^4 \hookrightarrow W^{2,\infty}$.

3.4. Error analysis. In this subsection, we shall derive some optimal error estimates for the proposed MIP-DG schemes (3.3)–(3.4), in which the constants in the error bounds depend on ϵ^{-1} only in low polynomial orders, instead of exponential orders. The key to obtaining such refined error bounds is to use the discrete spectrum estimate (3.20). In addition, a nonlinear Gronwall inequality from [13, Lemma 2.3] will be critically used in the proof. To ease the presentation, we set $r = 1$ in this subsection and section 4, and generalization to $r > 1$ can be proven similarly.

The main results of this subsection are stated in the following theorem.

THEOREM 3.5. *Let $\{(U^m, W^m)\}_{m=0}^M$ be the solution of scheme* (3.3)–(3.4) *with $r = 1$. Suppose that the general assumptions hold and $\sigma_e^0 > \sigma_*^0$ for all $e \in \mathcal{E}_h$, and define*

$$\rho_1(\epsilon, d) := \epsilon^{1-\frac{2}{6-d}\max\{2\sigma_1+5,2\sigma_3+2\}-\max\{2\sigma_1+\frac{13}{2},2\sigma_3+\frac{7}{2},2\sigma_2+4\}} + \epsilon^{-2\sigma_5} + \epsilon^{-\max\{2\sigma_1+7,2\sigma_3+4\}}, \tag{3.42}$$

$$\rho_3(\epsilon) := \epsilon^{-\max\{2\sigma_1+\frac{13}{2},2\sigma_3+\frac{7}{2},2\sigma_2+4,2\sigma_4\}-4}, \tag{3.43}$$

$$r_\epsilon(h, k) := k^2\rho_1(\epsilon; d) + h^6\rho_3(\epsilon). \tag{3.44}$$

Then, under the mesh and starting value conditions

$$h^{2-\frac{d}{2}} \le (C_1C_2)^{-1}\epsilon^{\max\{\sigma_1+\frac{11}{2},\sigma_3+4\}}, \tag{3.45}$$

$$h^{1+r}|\ln h|^{\bar r} \le (C_1C_3)^{-1}\epsilon^{\gamma+3}, \tag{3.46}$$

$$k \le \epsilon^3 \qquad \text{when } f^m = (U^m)^3 - U^m, \tag{3.47}$$

$$h^{2\theta} \le C\frac{\epsilon(1-\epsilon^3)}{8-4\epsilon^3} \quad \text{and} \quad k \le C\epsilon^{\frac{4(6+d)}{4-d}+(4d-2)\sigma_1}, \tag{3.48}$$

$$(U^0, 1) = (u_0, 1) \quad \text{and} \quad \|u_0 - U^0\|_{H^{-1}} \le Ch^3\|u_0\|_{H^2}, \tag{3.49}$$

there hold the error estimates

$$\max_{0\le m\le M}\|u(t_m)-U^m\|_{-1,h}+\Big(\sum_{m=1}^{M}k^2\|d_t(u(t_m)-U^m)\|_{-1,h}^2\Big)^{\frac12}\le Cr_\epsilon(h,k)^{\frac12}, \tag{3.50}$$

$$\Big(k\sum_{m=1}^{M}\|u(t_m)-U^m\|_{L^2}^2\Big)^{\frac12}\le C\Big(h^2\epsilon^{-\max\{\sigma_1+\frac52,\sigma_3+1\}}+\epsilon^{-2}r_\epsilon(h,k)^{\frac12}\Big), \tag{3.51}$$

$$\Big(k\sum_{m=1}^{M}|||u(t_m)-U^m|||_a^2\Big)^{\frac12}\le C\Big(h\epsilon^{-\max\{\sigma_1+\frac52,\sigma_3+1\}}+\epsilon^{-2}r_\epsilon(h,k)^{\frac12}\Big). \tag{3.52}$$

Moreover, if the starting value U^0 satisfies

$$\|u_0-U^0\|_{L^2}\le Ch^2\|u_0\|_{H^2}, \tag{3.53}$$

then there hold

$$\begin{aligned}\max_{0\le m\le M}\|u(t_m)-U^m\|_{L^2}&+\Big(k\sum_{m=1}^{M}k\|d_t(u(t_m)-U^m)\|_{L^2}^2\Big)^{\frac12}\\&+\Big(\frac{k}{\epsilon}\sum_{m=1}^{M}\|w(t_m)-W^m\|_{L^2}^2\Big)^{\frac12}\le C\Big(h^2\rho_3(\epsilon)^{\frac12}+\epsilon^{-\frac72}r_\epsilon(h,k)^{\frac12}\Big),\end{aligned} \tag{3.54}$$

$$\max_{0\le m\le M}\|u(t_m)-U^m\|_{L^\infty}\le C\Big(h^2|\ln h|\epsilon^{-\gamma}+h^{-\frac d2}\epsilon^{-\frac72}r_\epsilon(h,k)^{\frac12}\Big). \tag{3.55}$$

Furthermore, suppose that the starting value W^0 satisfies

$$\|P_hw_0-W^0\|_{L^2}\le Ch^\beta \tag{3.56}$$

for some $\beta>1$, and there exists a constant γ' such that

$$\operatorname*{ess\,sup}_{t\in[0,\infty)}\|w\|_{W^{2,\infty}}\le C\epsilon^{-\gamma'}; \tag{3.57}$$

then we have

$$\max_{0\le m\le M}\|w(t_m)-W^m\|_{L^2}\le C\big(h^2\rho_3(\epsilon)+h^\beta+k^{-\frac12}\epsilon^{-3}r_\epsilon(h,k)^{\frac12}\big), \tag{3.58}$$

$$\max_{0\le m\le M}\|w(t_m)-W^m\|_{L^\infty}\le C\big(h^{-\frac d2}\big(k^{-\frac12}\epsilon^{-3}r_\epsilon(h,k)^{\frac12}+h^\beta\big)+h^2|\ln h|\epsilon^{-\gamma'}\big). \tag{3.59}$$

Proof. In the following, we give a proof only for the convex splitting scheme corresponding to $f^m=(u^m)^3-u^{m-1}$ in (3.13) because the proof for the fully implicit scheme with $f^m=(u^m)^3-u^m$ is almost the same. We divide it into four steps.

Step 1. It is obvious that (1.1)–(1.4) imply that

$$\big(u_t(t_m),\eta_h\big)+a_h(w(t_m),\eta_h)=0 \qquad \forall\eta_h\in V_h, \tag{3.60}$$

$$\epsilon a_h(u(t_m),v_h)+\frac1\epsilon\big(f(u(t_m)),v_h\big)=\big(w(t_m),v_h\big) \qquad \forall v_h\in V_h. \tag{3.61}$$

Define error functions $E^m:=u(t_m)-U^m$ and $G^m:=w(t_m)-W^m$. Subtracting (3.3) from (3.60) and (3.4) from (3.61) yields the following error equations:

$$\big(d_tE^m,\eta_h\big)+a_h(G^m,\eta_h)=\big(R(u_{tt},m),\eta_h\big) \qquad \forall\eta_h\in V_h, \tag{3.62}$$

$$\epsilon a_h(E^m,v_h)+\frac1\epsilon\big(f(u(t_m))-f(U^m),v_h\big)=\big(G^m,v_h\big) \qquad \forall v_h\in V_h, \tag{3.63}$$

where $R(u_{tt};m) := \frac{1}{k}\int_{t_{m-1}}^{t_m}(s-t_{m-1})u_{tt}(s)\,ds$. It follows from solution estimates that

$$\begin{aligned} k\sum_{m=1}^{M}\|R(u_{tt};m)\|_{H^{-1}}^2 &\le \frac{1}{k}\sum_{m=1}^{M}\left(\int_{t_{m-1}}^{t_m}(s-t_{m-1})^2\,ds\right)\left(\int_{t_{m-1}}^{t_m}\|u_{tt}(s)\|_{H^{-1}}^2\,ds\right)\\ &\le Ck^2\rho_1(\epsilon,d). \end{aligned}$$

Introduce the error decompositions $E^m = \Theta^m + \Phi^m$ and $G^m = \Lambda^m + \Psi^m$, where

$$\begin{aligned} \Theta^m &:= u(t_m) - P_h u(t_m), &\qquad \Phi^m &:= P_h u(t_m) - U^m,\\ \Lambda^m &:= w(t_m) - P_h w(t_m), &\qquad \Psi^m &:= P_h w(t_m) - W^m. \end{aligned}$$

Using the definition of the operator P_h in (3.6), (3.62)–(3.63) can be rewritten as

$$\big(d_t\Phi^m,\eta_h\big) + a_h(\Psi^m,\eta_h) = -\big(d_t\Theta^m,\eta_h\big) + \big(R(u_{tt},m),\eta_h\big) \qquad \forall \eta_h\in V_h, \tag{3.64}$$

$$\epsilon a_h(\Phi^m,v_h) + \frac{1}{\epsilon}\big(f(u(t_m)) - f^m, v_h\big) = \big(\Psi^m,v_h\big) + \big(\Lambda^m,v_h\big) \qquad \forall v_h\in V_h. \tag{3.65}$$

Setting $\eta_h = -\Delta_h^{-1}\Phi^m$ in (3.64) and $v_h = \Phi^m$ in (3.65), adding the resulting equations, and summing over m from 1 to ℓ, we get

$$\begin{aligned} &a_h(\Delta_h^{-1}\Phi^\ell,\Delta_h^{-1}\Phi^\ell) + \sum_{m=1}^{\ell} a_h(\Delta_h^{-1}\Phi^m - \Delta_h^{-1}\Phi^{m-1},\Delta_h^{-1}\Phi^m - \Delta_h^{-1}\Phi^{m-1})\\ &\qquad + 2k\sum_{m=1}^{\ell}\epsilon a_h(\Phi^m,\Phi^m) + 2k\sum_{m=1}^{\ell}\frac{1}{\epsilon}\big(f(u(t_m)) - f^m,\Phi^m\big)\\ &= 2k\sum_{m=1}^{\ell}\Big(\big(R(u_{tt},m),-\Delta_h^{-1}\Phi^m\big) - \big(d_t\Theta^m,-\Delta_h^{-1}\Phi^m\big) + \big(\Lambda^m,\Phi^m\big)\Big)\\ &\qquad + a_h(\Delta_h^{-1}\Phi^0,\Delta_h^{-1}\Phi^0). \end{aligned} \tag{3.66}$$

Step 2. For $\sigma_e^0 > \sigma_*^e$ for all $e\in\mathcal{E}_h$, the first long term on the right-hand side of (3.66) can be bounded as follows:

$$\begin{aligned} &2k\sum_{m=1}^{\ell}\Big(\big(R(u_{tt},m),-\Delta_h^{-1}\Phi^m\big) + \big(d_t\Theta^m,-\Delta_h^{-1}\Phi^m\big) + \big(\Lambda^m,\Phi^m\big)\Big)\\ &\qquad \le k\sum_{m=1}^{\ell}\Big(a_h(\Delta_h^{-1}\Phi^m,\Delta_h^{-1}\Phi^m) + \frac{\epsilon^4}{1-\epsilon^3}a_h(\Phi^m,\Phi^m)\Big)\\ &\qquad\quad + C\Big(k^2\rho_1(\epsilon,d) + h^6\rho_3(\epsilon)\Big), \end{aligned} \tag{3.67}$$

where we have used the solution estimates and the facts [10]

$$\|u - P_h u\|_{H^{-1}} \le Ch^3\|u\|_{H^2}, \qquad \|w - P_h w\|_{H^{-1}} \le Ch^3\|w\|_{H^2}.$$

We now bound the last term on the left-hand side of (3.66). By the definition of f^m, we have

$$\begin{aligned} f(u(t_m)) - f^m &= f(u(t_m)) - f\big(P_h u(t_m)\big) + f\big(P_h u(t_m)\big) - f^m\\ &\ge -C|\Theta^m| + f'\big(P_h u(t_m)\big)\,\Phi^m - 3P_h u(t_m)\,(\Phi^m)^2 + (\Phi^m)^3 - kd_tU^m. \end{aligned}$$

By the discrete energy law (3.17), (3.13), and (3.38), we obtain for any $1 \le \ell \le M$

$$\begin{aligned}(3.68)\quad &2k\sum_{m=1}^{\ell}\frac{1}{\epsilon}\big(f(u(t_m)) - f^m, \Phi^m\big)\\ &\ge 2k\sum_{m=1}^{\ell}\frac{1}{\epsilon}\Big(f'\big(P_h u(t_m)\big), (\Phi^m)^2\Big) + \frac{2k}{\epsilon}\sum_{m=1}^{\ell}\|\Phi^m\|_{L^4}^4 - \frac{Ck}{\epsilon}\sum_{m=1}^{\ell}\|\Phi^m\|_{L^3}^3\\ &\quad - k\frac{\epsilon^4}{1-\epsilon^3}\sum_{m=1}^{\ell}a_h(\Phi^m,\Phi^m) - C\Big(h^6\epsilon^{-6}\|u\|^2_{L^2((0,T);H^s(\Omega))} + k^2\epsilon^{-6}E_h(U^0)\Big).\end{aligned}$$

Substituting (3.67) and (3.68) into (3.66) we get

$$\begin{aligned}(3.69)\quad &a_h(\Delta_h^{-1}\Phi^\ell, \Delta_h^{-1}\Phi^\ell) + \sum_{m=1}^{\ell}a_h(\Delta_h^{-1}\Phi^m - \Delta_h^{-1}\Phi^{m-1}, \Delta_h^{-1}\Phi^m - \Delta_h^{-1}\Phi^{m-1})\\ &\quad + \frac{2k(1-5\epsilon^3)}{1-\epsilon^3}\sum_{m=1}^{\ell}\Big(\epsilon a_h(\Phi^m,\Phi^m) + \frac{1-\epsilon^3}{\epsilon}\big(f'(P_h u(t_m))\Phi^m, \Phi^m\big)\Big)\\ &\quad + \frac{6\epsilon^4}{1-\epsilon^3}k\sum_{m=1}^{\ell}a_h(\Phi^m,\Phi^m) + \frac{2k}{\epsilon}\sum_{m=1}^{\ell}\|\Phi^m\|_{L^4}^4\\ &\le Ck\sum_{m=1}^{\ell}a_h(\Delta_h^{-1}\Phi^m, \Delta_h^{-1}\Phi^m) + \frac{Ck}{\epsilon}\sum_{m=1}^{\ell}\|\Phi^m\|_{L^3}^3\\ &\quad - Ck\epsilon^2\sum_{m=1}^{\ell}\big(f'(P_h u(t_m))\Phi^m, \Phi^m\big) + C\big(k^2\rho_1(\epsilon; d) + h^6\rho_3(\epsilon)\big)\\ &\quad + C\Big(h^6\epsilon^{-6}\|u\|^2_{L^2((0,T);H^s(\Omega)} + k^2\epsilon^{-6}E_h(U^0)\Big).\end{aligned}$$

Step 3. To control the second term on the right-hand side of (3.69), we appeal to the following Gagliardo–Nirenberg inequality [1]:

$$\|v\|^3_{L^3(K)} \le C\Big(\|\nabla v\|^{\frac{d}{2}}_{L^2(K)}\|v\|^{\frac{6-d}{2}}_{L^2(K)} + \|v\|^3_{L^2(K)}\Big) \qquad \forall K \in \mathcal{T}_h.$$

Thus we get

$$\begin{aligned}(3.70)\quad \frac{Ck}{\epsilon}\sum_{m=1}^{\ell}\|\Phi^m\|^3_{L^3} &\le \epsilon^4 k\sum_{m=1}^{\ell}\|\nabla\Phi^m\|^2_{L^2(\mathcal{T}_h)} + \frac{Ck}{\epsilon}\sum_{m=1}^{\ell}\|\Phi^m\|^3_{L^2}\\ &\quad + C\epsilon^{-\frac{4(1+d)}{4-d}}k\sum_{m=1}^{\ell}\big\|\Phi^m\big\|_{L^2}^{\frac{2(6-d)}{4-d}}\\ &\le k\sum_{m=1}^{\ell}\Big(\frac{\epsilon^4}{1-\epsilon^3}a_h(\Phi^m,\Phi^m) + \frac{C}{\epsilon}\|\Phi^m\|^3_{L^2} + C\epsilon^{-\frac{4(1+d)}{4-d}}\big\|\Phi^m\big\|_{L^2}^{\frac{2(6-d)}{4-d}}\Big).\end{aligned}$$

The third item on the right-hand side of (3.69) can be bounded by

$$(3.71)\quad -C(f'(P_h u(t_m))\Phi^m, \Phi^m) \le \frac{\epsilon^2}{1-\epsilon^3}a_h(\Phi^m,\Phi^m) + \frac{C}{\epsilon^2}a_h(\Delta_h^{-1}\Phi^m, \Delta_h^{-1}\Phi^m).$$

Again, here we have used (3.38).

Finally, for the third term on the left-hand side of (3.69), we utilize the discrete spectrum estimate (3.20) to bound it from below as follows:

$$\epsilon a_h(\Phi^m,\Phi^m)+\frac{1-\epsilon^3}{\epsilon}\big(f'(P_h u(t_m))\Phi^m,\Phi^m\big)\geq -c_0\|\nabla\Delta^{-1}\Phi^m\|_{L^2}^2. \tag{3.72}$$

By the stability of Δ^{-1} and (3.38), we also have

$$c_0\|\nabla\Delta^{-1}\Phi^m\|_{L^2}^2\leq C\|\Phi^m\|_{L^2}^2\leq \frac{\epsilon^4}{1-\epsilon^3}a_h(\Phi^m,\Phi^m)+Ca_h(\Delta_h^{-1}\Phi^m,\Delta_h^{-1}\Phi^m). \tag{3.73}$$

Step 4. Substituting (3.70), (3.71), (3.72), (3.73) into (3.69), we get

$$\begin{aligned} &a_h(\Delta_h^{-1}\Phi^\ell,\Delta_h^{-1}\Phi^\ell)+\sum_{m=1}^{\ell}a_h(\Delta_h^{-1}\Phi^m-\Delta_h^{-1}\Phi^{m-1},\Delta_h^{-1}\Phi^m-\Delta_h^{-1}\Phi^{m-1})\\ &\qquad+\frac{2\epsilon^4 k}{1-\epsilon^3}\sum_{m=1}^{\ell}a_h(\Phi^m,\Phi^m)+\frac{2k}{\epsilon}\sum_{m=1}^{\ell}\|\Phi^m\|_{L^4}^4\\ &\leq Ck\sum_{m=1}^{\ell}a_h(\Delta_h^{-1}\Phi^m,\Delta_h^{-1}\Phi^m)+\frac{Ck}{\epsilon}\sum_{m=1}^{\ell}\|\Phi^m\|_{L^2}^3\\ &\quad+C\epsilon^{-\frac{4(1+d)}{4-d}}k\sum_{m=1}^{\ell}\big\|\Phi^m\big\|_{L^2}^{\frac{2(6-d)}{4-d}}+C\big(k^2\rho_1(\epsilon;d)+h^6\rho_3(\epsilon)\big)\\ &\quad+C\Big(h^6\epsilon^{-6}\|u\|_{L^2((0,T);H^s(\Omega))}^2+k^2\epsilon^{-6}E_h(U^0)\Big). \end{aligned} \tag{3.74}$$

By the discrete energy law (3.17), general assumption (2.3), H^1 stability of elliptic projection, L^∞ stability (or L^∞ error estimate and triangle inequality) of elliptic projection, we have $\|U^\ell\|_{L^2}\leq C\epsilon^{-\sigma_1}$ for $0\leq\ell\leq M$. Since the projection of u is bounded, then we get $\|\Phi^\ell\|_{L^2}\leq C\epsilon^{-\sigma_1}$ for $0\leq\ell\leq M$. Because the exponent for $\big\|\Phi^m\big\|_{L^2}$ is $\frac{2(6-d)}{4-d}$, which is bigger than 3 for $d=2,3$, therefore

$$\big\|\Phi^m\big\|_{L^2}^4\leq C\epsilon^{-\sigma_1}\big\|\Phi^m\big\|_{L^2}^3,\qquad \big\|\Phi^m\big\|_{L^2}^6\leq C\epsilon^{-3\sigma_1}\big\|\Phi^m\big\|_{L^2}^3.$$

By the Schwarz and Young's inequalities, we have

$$\begin{aligned} \big\|\Phi^m\big\|_{L^2}^3&=a_h(-\Delta_h^{-1}\Phi^m,\Phi^m)^{\frac32}\leq a_h(\Delta_h^{-1}\Phi^m,\Delta_h^{-1}\Phi^m)^{\frac34}\,a_h(\Phi^m,\Phi^m)^{\frac34}\\ &\leq \epsilon^{\frac{4(1+d)}{4-d}+(2d-3)\sigma_1}\frac{\epsilon^4}{1-\epsilon^3}a_h(\Phi^m,\Phi^m)\\ &\qquad+C\epsilon^{-4}\epsilon^{-\frac{4(1+d)}{4-d}-(2d-3)\sigma_1}a_h(\Delta_h^{-1}\Phi^m,\Delta_h^{-1}\Phi^m)^3. \end{aligned} \tag{3.75}$$

Therefore, (3.74) becomes

$$\begin{aligned} &a_h(\Delta_h^{-1}\Phi^\ell,\Delta_h^{-1}\Phi^\ell)+\sum_{m=1}^{\ell}a_h(\Delta_h^{-1}\Phi^m-\Delta_h^{-1}\Phi^{m-1},\Delta_h^{-1}\Phi^m-\Delta_h^{-1}\Phi^{m-1})\\ &\qquad+\frac{\epsilon^4 k}{1-\epsilon^3}\sum_{m=1}^{\ell}a_h(\Phi^m,\Phi^m)+\frac{2k}{\epsilon}\sum_{m=1}^{\ell}\|\Phi^m\|_{L^4}^4 \end{aligned} \tag{3.76}$$

$$
\begin{aligned}
&\leq Ck\sum_{m=1}^{\ell} a_h(\Delta_h^{-1}\Phi^m, \Delta_h^{-1}\Phi^m) + C\big(k^2\rho_1(\epsilon;d) + h^6\rho_3(\epsilon)\big)\\
&\qquad + Ck\epsilon^{-\frac{4(6+d)}{4-d}-(4d-6)\sigma_1}\sum_{m=1}^{\ell} a_h(\Delta_h^{-1}\Phi^m, \Delta_h^{-1}\Phi^m)^3.
\end{aligned}
$$

By (2.3) and (3.17), we get

$$
\|U^\ell\|_{-1,h} \leq k\sum_{m=1}^{\ell}\|d_tU^m\|_{-1,h} + \|U^0\|_{-1,h} \leq C\epsilon^{-\sigma_1}. \tag{3.77}
$$

Using the boundedness of the projection, we obtain $\|\Phi^\ell\|_{-1,h}^2 \leq C\epsilon^{-2\sigma_1}$. Also, (3.76) can be written in the following equivalent form:

$$
\begin{aligned}
&a_h(\Delta_h^{-1}\Phi^\ell, \Delta_h^{-1}\Phi^\ell) + \sum_{m=1}^{\ell} a_h(\Delta_h^{-1}\Phi^m - \Delta_h^{-1}\Phi^{m-1}, \Delta_h^{-1}\Phi^m - \Delta_h^{-1}\Phi^{m-1})\\
&\qquad + \frac{\epsilon^4 k}{1-\epsilon^3}\sum_{m=1}^{\ell} a_h(\Phi^m, \Phi^m) + \frac{2k}{\epsilon}\sum_{m=1}^{\ell}\|\Phi^m\|_{L^4}^4 \leq M_1 + M_2,
\end{aligned} \tag{3.78}
$$

where

$$
\begin{aligned}
M_1 &:= Ck\sum_{m=1}^{\ell-1} a_h(\Delta_h^{-1}\Phi^m, \Delta_h^{-1}\Phi^m) + C\big(k^2\rho_1(\epsilon;d) + h^6\rho_3(\epsilon)\big)\\
&\qquad + Ck\epsilon^{-\frac{4(6+d)}{4-d}-(4d-6)\sigma_1}\sum_{m=1}^{\ell-1} a_h(\Delta_h^{-1}\Phi^m, \Delta_h^{-1}\Phi^m)^3,
\end{aligned} \tag{3.79}
$$

$$
M_2 := Cka_h(\Delta_h^{-1}\Phi^\ell, \Delta_h^{-1}\Phi^\ell) + Ck\epsilon^{-\frac{4(6+d)}{4-d}-(4d-6)\sigma_1} a_h(\Delta_h^{-1}\Phi^\ell, \Delta_h^{-1}\Phi^\ell)^3. \tag{3.80}
$$

It is easy to check that

$$
M_2 \leq \frac{1}{2}\|\Phi^\ell\|_{-1,h}^2 \qquad \text{provided that} \quad k \leq C\epsilon^{\frac{4(6+d)}{4-d}+(4d-6)\sigma_1}. \tag{3.81}
$$

Under this restriction, we have

$$
\begin{aligned}
&a_h(\Delta_h^{-1}\Phi^\ell, \Delta_h^{-1}\Phi^\ell) + 2\sum_{m=1}^{\ell} a_h(\Delta_h^{-1}\Phi^m - \Delta_h^{-1}\Phi^{m-1}, \Delta_h^{-1}\Phi^m - \Delta_h^{-1}\Phi^{m-1})\\
&\qquad + \frac{2\epsilon^4 k}{1-\epsilon^3}\sum_{m=1}^{\ell} a_h(\Phi^m, \Phi^m) + \frac{4k}{\epsilon}\sum_{m=1}^{\ell}\|\Phi^m\|_{L^4}^4\\
&\leq Ck\sum_{m=1}^{\ell-1} a_h(\Delta_h^{-1}\Phi^m, \Delta_h^{-1}\Phi^m) + C\big(k^2\rho_1(\epsilon;d) + h^6\rho_3(\epsilon)\big)\\
&\qquad + Ck\epsilon^{-\frac{4(6+d)}{4-d}-(4d-6)\sigma_1}\sum_{m=1}^{\ell-1} a_h(\Delta_h^{-1}\Phi^m, \Delta_h^{-1}\Phi^m)^3.
\end{aligned} \tag{3.82}
$$

Define the slack variable $d_\ell \geq 0$ such that

$$
\begin{aligned}
(3.83)\quad & a_h(\Delta_h^{-1}\Phi^\ell, \Delta_h^{-1}\Phi^\ell) + 2\sum_{m=1}^{\ell} a_h(\Delta_h^{-1}\Phi^m - \Delta_h^{-1}\Phi^{m-1}, \Delta_h^{-1}\Phi^m - \Delta_h^{-1}\Phi^{m-1}) \\
&\qquad + \frac{2\epsilon^4 k}{1-\epsilon^3}\sum_{m=1}^{\ell} a_h(\Phi^m, \Phi^m) + \frac{4k}{\epsilon}\sum_{m=1}^{\ell}\|\Phi^m\|_{L^4}^4 + d_\ell \\
&= Ck\sum_{m=1}^{\ell-1} a_h(\Delta_h^{-1}\Phi^m, \Delta_h^{-1}\Phi^m) + C\big(k^2\rho_1(\epsilon; d) + h^6\rho_3(\epsilon)\big) \\
&\quad + Ck\epsilon^{-\frac{4(6+d)}{4-d}-(4d-6)\sigma_1}\sum_{m=1}^{\ell-1} a_h(\Delta_h^{-1}\Phi^m, \Delta_h^{-1}\Phi^m)^3.
\end{aligned}
$$

We also define $\{S_\ell\}_{\ell\geq 1}$ by

$$
\begin{aligned}
(3.84)\quad S_\ell = d_\ell &+ 2\sum_{m=1}^{\ell} a_h(\Delta_h^{-1}\Phi^m - \Delta_h^{-1}\Phi^{m-1}, \Delta_h^{-1}\Phi^m - \Delta_h^{-1}\Phi^{m-1}) \\
&+ a_h(\Delta_h^{-1}\Phi^\ell, \Delta_h^{-1}\Phi^\ell) + \frac{2\epsilon^4 k}{1-\epsilon^3}\sum_{m=1}^{\ell} a_h(\Phi^m, \Phi^m) + \frac{4k}{\epsilon}\sum_{m=1}^{\ell}\|\Phi^m\|_{L^4}^4,
\end{aligned}
$$

and (3.83) implies that $S_1 = C\big(k^2\rho_1(\epsilon; d) + h^6\rho_3(\epsilon)\big)$. Then

$$
(3.85)\qquad S_{\ell+1} - S_\ell \leq CkS_\ell + Ck\epsilon^{-\frac{4(6+d)}{4-d}-(4d-6)\sigma_1}S_\ell^3 \qquad \forall \ell \geq 1.
$$

Applying Lemma 2.3 of [13] to $\{S_\ell\}_{\ell\geq 1}$ defined above, we obtain for all $\ell \geq 1$

$$
(3.86)\qquad S_\ell \leq a_\ell^{-1}\left\{S_1^{-2} - 2C\epsilon^{-\frac{4(6+d)}{4-d}-(4d-6)\sigma_1}k\sum_{s=1}^{\ell-1}a_{s+1}^{-2}\right\}^{-\frac{1}{2}}
$$

provided that

$$
(3.87)\qquad S_1^{-2} - 2C\epsilon^{-\frac{4(6+d)}{4-d}-(4d-6)\sigma_1}k\sum_{s=1}^{\ell-1}a_{s+1}^{-2} > 0.
$$

We note that $a_s\ (1 \leq s \leq \ell)$ are all bounded as $k \to 0$, and therefore (3.87) holds under the mesh constraint stated in the theorem. It follows from (3.49) that

$$
(3.88)\qquad S_\ell \leq 2a_\ell^{-1}S_1 \leq C\big(k^2\rho_1(\epsilon; d) + h^6\rho_3(\epsilon)\big).
$$

Then (3.50) follows from the triangle inequality on $E^m = \Theta^m + \Phi^m$. Equation (3.52) can be obtained by (3.84) and (3.88), and (3.51) is a consequence of the Poincaré inequality.

Now setting $\eta_h = \Phi^m$ in (3.64) and $v_h = -\Psi^m/\epsilon$ in (3.65) and adding the resulting equations yields

$$
\begin{aligned}
(3.89)\quad \frac{1}{2}d_t\|\Phi^m\|_{L^2}^2 + \frac{k}{2}\|d_t\Phi^m\|_{L^2}^2 + \frac{1}{\epsilon}\|\Psi^m\|_{L^2}^2 &= \frac{1}{\epsilon^2}\big(f(u(t_m)) - f(U^m), \Psi^m\big) \\
&\quad + \big(R(u_{tt}; m), \Phi^m\big) - \big(d_t\Theta^m, \Phi^m\big) - \frac{1}{\epsilon}\big(\Lambda^m, \Psi^m\big).
\end{aligned}
$$

The last three terms on the right-hand side of (3.89) can be bounded in the same way as in (3.67), and the first term can be controlled as

$$\frac{1}{\epsilon^2}\big(f(u(t_m)) - f(U^m), \Psi^m\big) = \frac{1}{\epsilon^2}\big(f'(\xi)E^m, \Psi^m\big) \le \frac{1}{2\epsilon}\|\Psi^m\|_{L^2}^2 + \frac{C}{\epsilon^3}\|E^m\|_{L^2}^2, \tag{3.90}$$

where we have used the fact that

$$\max_{0\le m\le M}\|U^m\|_{L^\infty} \le C, \tag{3.91}$$

and the details can be found in [14]. Multiplying both sides of (3.89) by k and summing over m from 1 to M yield the desired estimate (3.54). Estimate (3.55) follows from an application of the inverse inequality $\|\Phi^m\|_{L^\infty} \le h^{-\frac{d}{2}}\|\Phi^m\|_{L^2}$ and the following L^∞ estimate:

$$\|u - P_h u\|_{L^\infty} \le Ch^2|\ln h|\|u\|_{W^{s,\infty}} \qquad \forall u \in H^2(\Omega). \tag{3.92}$$

Finally, it is well known that the following estimate holds:

$$\max_{0\le m\le M}\|\Lambda^m\|_{L^2} + \left(k\sum_{m=0}^{M} k\|d_t\Lambda^m\|_{L^2}^2\right)^{\frac12} \le Ch^2\rho_2(\epsilon) \tag{3.93}$$

with $\rho_2(\epsilon) = \epsilon^{-\max\{\sigma_1+5,\sigma_3+\frac72,\sigma_2+\frac52,\sigma_4+1\}}$. Using the identity

$$\big(d_t\Phi^m, \Phi^m\big) = \frac12 d_t\|\Phi^m\|_{L^2}^2 + \frac{k}{2}\|d_t\Phi^m\|_{L^2}^2, \tag{3.94}$$

we get

$$\begin{aligned}\frac12\|\Psi^M\|_{L^2}^2 + k\sum_{m=1}^{M}\frac{k}{2}\|d_t\Psi^m\|_{L^2}^2 &= k\sum_{m=1}^{M}\big(d_t\Psi^m, \Psi^m\big) + \frac12\|\Psi^0\|_{L^2}^2 \\ &\le k\sum_{m=1}^{M}\left(\frac{k}{4}\|d_t\Psi^m\|_{L^2}^2 + \frac1k\|\Psi^m\|_{L^2}^2\right) + \frac12\|\Psi^0\|_{L^2}^2.\end{aligned} \tag{3.95}$$

The first term on the right-hand side of (3.95) can be absorbed by the second term on the left-hand side of (3.95). The second tern on the right-hand side of (3.95) has been obtained in (3.54). Estimate (3.58) for W^m then follows from (3.93) and (3.95). Equation (3.59) follows from an application of the triangle inequality, the inverse inequality, and (3.92). This completes the proof. ∎

4. Convergence of numerical interfaces. In this section, we prove that the numerical interface defined as the zero-level set of the finite element interpolation of the solution U^m converges to the moving interface of the Hele–Shaw problem under the assumption that the Hele–Shaw problem has a unique global (in time) classical solution. To this end, we first cite the following PDE convergence result proved in [2].

THEOREM 4.1. *Let Ω be a given smooth domain and Γ_{00} be a smooth closed hypersurface in Ω. Suppose that the Hele–Shaw problem starting from Γ_{00} has a unique smooth solution $\big(w, \Gamma := \bigcup_{0\le t\le T}(\Gamma_t \times \{t\})\big)$ in the time interval $[0,T]$ such that $\Gamma_t \subseteq \Omega$ for all $t \in [0,T]$. Then there exists a family of smooth functions $\{u_0^\epsilon\}_{0<\epsilon\le1}$ which are uniformly bounded in $\epsilon \in (0,1]$ and $(x,t) \in \overline{\Omega}_T$ such that if u^ϵ solves the Cahn–Hilliard problem* (1.1)–(1.5)*, then*

(i) $\lim_{\epsilon\to 0} u^\epsilon(x,t) = \begin{cases} 1 & if (x,t)\in\mathcal{O} \\ -1 & if (x,t)\in\mathcal{I} \end{cases}$ *uniformly on compact subsets, where $\mathcal{I}$ and $\mathcal{O}$ stand for the "inside" and "outside" of Γ;*

(ii) $\lim_{\epsilon\to 0}\big(\epsilon^{-1} f(u^\epsilon) - \epsilon\Delta u^\epsilon\big)(x,t) = -w(x,t)$ *uniformly on $\overline{\Omega}_T$.*

We note that since U^m is multivalued on the edges of the mesh $\mathcal{T}_h$, its zero-level set is not well defined. To avoid this technicality, we use a continuous finite element interpolation of U^m to define the numerical interface. Let $\widehat{U}^m \in S_h$ denote the finite element approximation of U^m which is defined using the averaged degrees of freedom of U^m as the degrees of freedom for determining $\widehat{U}^m$ (cf. [18]).

By the construction, $\widehat{U}^m$ is expected to be very close to U^m; hence, $\widehat{U}^m$ should also be very close to $u(t_m)$. This is indeed the case as stated in the following theorem, which says that Theorem 3.5 also holds for $\widehat{U}^m$.

THEOREM 4.2. *Let U^m denote the solution of scheme* (3.1)–(3.14) *and $\widehat{U}^m$ denote its finite element approximation as defined above. Then under the assumptions of Theorem* 3.5 *the error estimates for U^m given in Theorem* 3.5 *are still valid for $\widehat{U}^m$; in particular, there holds*

$$\max_{0\le m\le M} \|u(t_m) - \widehat{U}^m\|_{L^\infty(\mathcal{T}_h)} \le C\Big(h^2|\ln h|\epsilon^{-\gamma} + h^{-\frac{d}{2}}\epsilon^{-\frac{7}{2}} r(h,k;\epsilon,d,\sigma_i)^{\frac12}\Big). \tag{4.1}$$

We omit the proof to save space and refer the reader to [13] to see a proof of the same nature for the related Allen–Cahn problem.

We are now ready to state the first main theorem of this section.

THEOREM 4.3. *Let $\{\Gamma_t\}_{t\ge 0}$ denote the zero-level set of the Hele–Shaw problem and $\big(U_{\epsilon,h,k}(x,t), W_{\epsilon,h,k}(x,t)\big)$ denote the piecewise linear interpolation in time of the finite element interpolation $\{(\widehat{U}^m, \widehat{W}^m)\}$ of the DG solution $\{(U^m, W^m)\}$, namely,*

$$U_{\epsilon,h,k}(x,t) := \frac{t-t_{m-1}}{k}\widehat{U}^m(x) + \frac{t_m - t}{k}\widehat{U}^{m-1}(x), \tag{4.2}$$

$$W_{\epsilon,h,k}(x,t) := \frac{t-t_{m-1}}{k}W^m(x) + \frac{t_m - t}{k}W^{m-1}(x), \tag{4.3}$$

for $t_{m-1}\le t\le t_m$ and $1\le m\le M$. Then, under the mesh and starting value constraints of Theorem 3.5 *and $k = O(h^{2-\gamma})$ with $\gamma>0$, we have the following:*

(i) $U_{\epsilon,h,k}(x,t) \overset{\epsilon\searrow 0}{\longrightarrow} 1$ *uniformly on compact subset of $\mathcal{O}$.*

(ii) $U_{\epsilon,h,k}(x,t) \overset{\epsilon\searrow 0}{\longrightarrow} -1$ *uniformly on compact subset of $\mathcal{I}$.*

(iii) *Moreover, in the case that dimension $d = 2$, when $k = O(h^3)$, suppose that W^0 satisfies $\|w_0^\epsilon - W^0\|_{L^2} \le Ch^\beta$ for some $\beta > \frac32$; then we have $W_{\epsilon,h,k}(x,t) \overset{\epsilon\searrow 0}{\longrightarrow} -w(x,t)$ uniformly on $\overline{\Omega}_T$.*

Proof. For any compact set $A\subset\mathcal{O}$ and for any $(x,t)\in A$, we have

$$\begin{aligned} |U_{\epsilon,h,k} - 1| &\le |U_{\epsilon,h,k} - u^\epsilon(x,t)| + |u^\epsilon(x,t) - 1| \\ &\le |U_{\epsilon,h,k} - u^\epsilon(x,t)|_{L^\infty(\Omega_T)} + |u^\epsilon(x,t) - 1|. \end{aligned} \tag{4.4}$$

Equation (3.55) of Theorem 3.5 infers that there exists a constant $0 < \alpha < \frac{4-d}{2}$ such that

$$|U_{\epsilon,h,k} - u^\epsilon(x,t)|_{L^\infty(\Omega_T)} \le Ch^\alpha. \tag{4.5}$$

The first term on the right-hand side of (4.4) tends to 0 when $\epsilon \searrow 0$ (note that $h, k \searrow 0$, too). The second term converges uniformly to 0 on the compact set A, which is ensured by (i) of Theorem 4.1. Hence, assertion (i) holds.

To show (ii), we only need to replace $\mathcal{O}$ by $\mathcal{I}$ and 1 by -1 in the above proof. To prove (iii), under the assumption $k = O(h^3)$, (3.59) in Theorem 3.5 implies that there exists a positive constant $0 < \zeta < \frac{4-d}{2}$ such that

$$\|W_{\epsilon,h,k} - w^\epsilon\|_{L^\infty(\Omega_T)} \le Ch^\zeta. \tag{4.6}$$

Then by the triangle inequality we obtain for any $(x,t) \in \overline{\Omega}_T$,

$$\begin{aligned} |W_{\epsilon,h,k}(x,t) - (-w)| &\le |W_{\epsilon,h,k}(x,t) - w^\epsilon(x,t)| + |w^\epsilon(x,t) - (-w)|, \\ &\le \|W_{\epsilon,h,k}(x,t) - w^\epsilon(x,t)\|_{L^\infty(\Omega_T)} + |w^\epsilon(x,t) - (-w)|. \end{aligned} \tag{4.7}$$

The first term on the right-hand side of (4.7) tends to 0 when $\epsilon \searrow 0$ (note that $h, k \searrow 0$, too). The second term converges uniformly to 0 in $\overline{\Omega}_T$, which is ensured by (ii) of Theorem 4.1. Thus assertion (iii) is proved. The proof is complete. ∎

The second main theorem of this section, which is given below, addresses the convergence of numerical interfaces.

THEOREM 4.4. *Let* $\Gamma_t^{\epsilon,h,k} := \{x \in \Omega;\, U_{\epsilon,h,k}(x,t) = 0\}$ *be the zero-level set of* $U_{\epsilon,h,k}(x,t)$*; then under the assumptions of Theorem* 4.3*, we have*

$$\sup_{x\in\Gamma_t^{\epsilon,h,k}} \operatorname{dist}(x,\Gamma_t) \xrightarrow{\epsilon\searrow 0} 0 \quad \textit{uniformly on } [0,T].$$

Proof. For any $\eta \in (0,1)$, define the tabular neighborhood $\mathcal{N}_\eta$ of width 2η of Γ_t

$$\mathcal{N}_\eta := \{(x,t) \in \Omega_T;\, \operatorname{dist}(x,\Gamma_t) < \eta\}. \tag{4.8}$$

Let A and B denote the complements of the neighborhood $\mathcal{N}_\eta$ in $\mathcal{O}$ and $\mathcal{I}$, respectively:

$$A = \mathcal{O} \setminus \mathcal{N}_\eta \qquad \text{and} \qquad B = \mathcal{I} \setminus \mathcal{N}_\eta.$$

Note that A is a compact subset outside Γ_t and B is a compact subset inside Γ_t; then there exists $\epsilon_3 > 0$, which only depends on η, such that for any $\epsilon \in (0, \epsilon_3)$

$$|U_{\epsilon,h,k}(x,t) - 1| \le \eta \quad \forall (x,t) \in A, \tag{4.9}$$

$$|U_{\epsilon,h,k}(x,t) + 1| \le \eta \quad \forall (x,t) \in B. \tag{4.10}$$

Now for any $t \in [0,T]$ and $x \in \Gamma_t^{\epsilon,h,k}$, from $U_{\epsilon,h,k}(x,t) = 0$ we have

$$|U_{\epsilon,h,k}(x,t) - 1| = 1 \qquad \forall (x,t) \in A, \tag{4.11}$$

$$|U_{\epsilon,h,k}(x,t) + 1| = 1 \qquad \forall (x,t) \in B. \tag{4.12}$$

Equations (4.9) and (4.11) imply that (x,t) is not in A, and (4.10) and (4.12) imply that (x,t) is not in B; then (x,t) must lie in the tubular neighborhood $\mathcal{N}_\eta$. Therefore, for any $\epsilon \in (0, \epsilon_3)$,

$$\sup_{x\in\Gamma_t^{\epsilon,h,k}} \operatorname{dist}(x,\Gamma_t) \le \eta \qquad \text{uniformly on } [0,T]. \tag{4.13}$$

The proof is complete. ∎

5. Numerical experiments. In this section, we present two two-dimensional numerical tests to gauge the performance of the proposed fully discrete MIP-DG methods using the linear element (i.e., $r = 1$). The square domain $\Omega = [-1,1]^2$ is used in both tests and the initial condition is chosen to have the form $u_0 = \tanh\big(\frac{d_0(x)}{\sqrt{2}\epsilon}\big)$, where $d_0(x)$ denotes the signed distance from x to the initial interface Γ_0.

Our first test uses a smooth initial condition to satisfy the requirement for u_0; consequently, the theoretical results established in this paper apply to this test problem. On the other hand, a nonsmooth initial condition is used in the second test, and hence the theoretical results of this paper may not apply. But we still use our MIP-DG methods to compute the error order, the energy decay, and the evolution of the numerical interfaces. Our numerical results suggest that the proposed DG schemes work well, even though a convergence result is missing for them.

Test 1. Consider the Cahn–Hilliard problem (1.1)–(1.5) with the following initial condition:

$$u_0(x) = \tanh\Big(\frac{d_0(x)}{\sqrt{2}\epsilon}\Big), \tag{5.1}$$

where $\tanh(t) = (e^t - e^{-t})/(e^t + e^{-t})$, and $d_0(x)$ represents the signed distance function to the ellipse $\frac{x_1^2}{0.36} + \frac{x_2^2}{0.04} = 1$. Hence, u_0 has the desired form as stated in Proposition 3.4.

Table 5.1
Spatial errors and convergence rates of Test 1 with $\epsilon = 0.1$.

	$L^\infty(L^2)$ error	$L^\infty(L^2)$ order	$L^2(H^1)$ error	$L^2(H^1)$ order
$h = 0.4\sqrt{2}$	0.53325		0.84260	
$h = 0.2\sqrt{2}$	0.21280	1.3253	0.64843	0.3779
$h = 0.1\sqrt{2}$	0.07164	1.5707	0.43273	0.5835
$h = 0.05\sqrt{2}$	0.01779	2.0097	0.21411	1.0151
$h = 0.025\sqrt{2}$	0.00454	1.9703	0.10890	0.9753

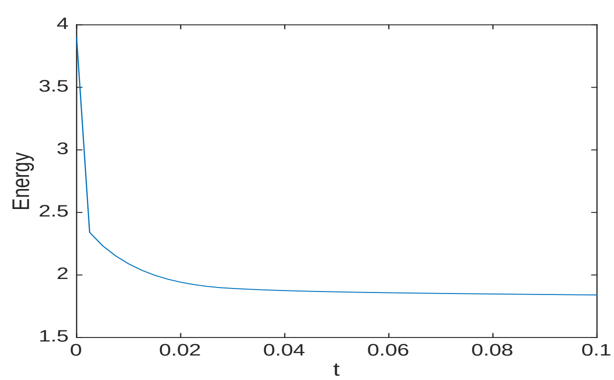

Fig. 5.1. *Decay of the numerical energy $E_h(U^\ell)$ of Test 1.*

Table 5.1 shows the spatial L^2 and H^1 norm errors and convergence rates, which are consistent with what are proved for the linear element in the convergence theorem. $\epsilon = 0.1$ is used to generate the table.

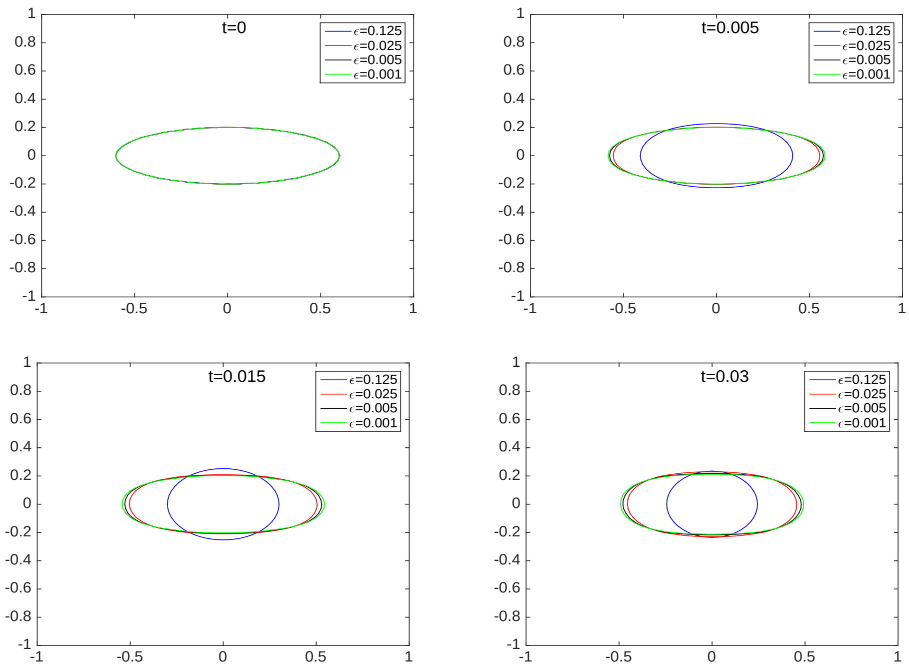

FIG. 5.2. *Test 1: Snapshots of the zero-level set of* $u^{\epsilon,h,k}$ *at time* $t = 0, 0.005, 0.015, 0.03$ *and* $\epsilon = 0.125, 0.025, 0.005, 0.001$.

TABLE 5.2
Spatial errors and convergence rates of Test 2 with $\epsilon = 0.1$.

	$L^\infty(L^2)$ error	$L^\infty(L^2)$ order	$L^2(H^1)$ error	$L^2(H^1)$ order
$h = 0.4\sqrt{2}$	0.26713		0.35714	
$h = 0.2\sqrt{2}$	0.07161	1.8993	0.18411	0.9559
$h = 0.1\sqrt{2}$	0.01833	1.9660	0.09620	0.9365
$h = 0.05\sqrt{2}$	0.00476	1.9452	0.04928	0.9650
$h = 0.025\sqrt{2}$	0.00121	1.9760	0.02497	0.9808

Figure 5.1 plots the change of the discrete energy $E_h(U^\ell)$ in time, which should decrease according to (3.17). This graph clearly confirms this decay property. Figure 5.2 displays four snapshots at four fixed time points of the numerical interface with four different ϵ. They clearly indicate that at each time point the numerical interface converges to the sharp interface Γ_t of the Hele–Shaw flow as ϵ tends to zero. It also shows that the numerical interface evolves faster in time for larger ϵ and confirms the mass conservation property of the Cahn–Hilliard problem as the total mass $m = \int_\Omega u\,dx$ equals a constant value 3.064 when $\epsilon = 0.125$.

Test 2. Consider the Cahn–Hilliard problem (1.1)–(1.5) with the following initial condition:

$$u_0(x) = \tanh\Big(\frac{1}{\sqrt{2}\epsilon}\big(\min\{\sqrt{(x_1+0.3)^2+x_2^2}-0.3, \sqrt{(x_1-0.3)^2+x_2^2}-0.25\}\big)\Big).$$

We note that u_0 can be written in the form given in (5.1) with $d_0(x)$ being the signed

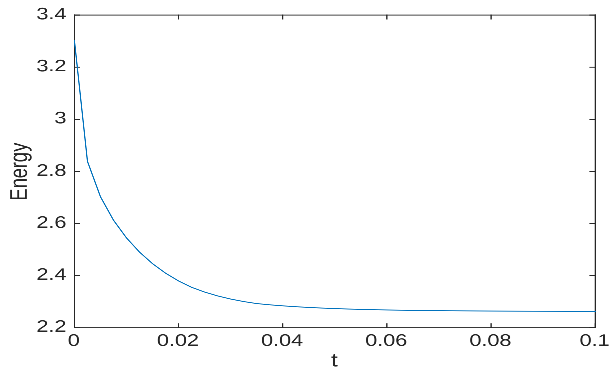

FIG. 5.3. *Decay of the numerical energy* $E_h(U^\ell)$ *of Test* 2.

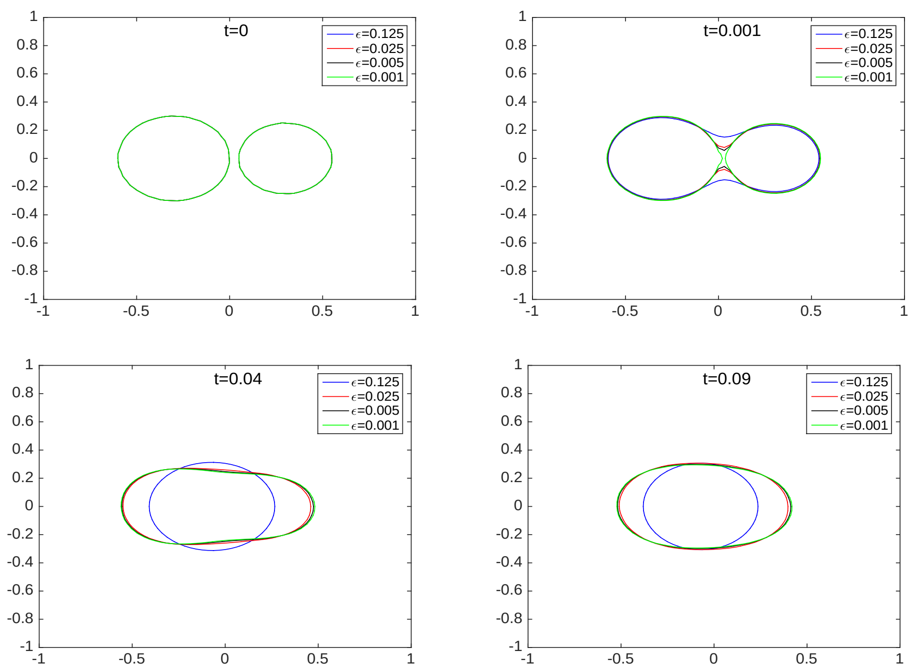

FIG. 5.4. *Test 2: Snapshots of the zero-level set of* $u^{\epsilon,h,k}$ *at time* $t = 0, 0.001, 0.04, 0.09$ *and* $\epsilon = 0.125, 0.025, 0.005, 0.001$.

distance function to the initial curve. We note that u_0 does not have the desired form as stated in Proposition 3.4.

Table 5.2 shows the spatial L^2 and H^1 norm errors and convergence rates, which are consistent with what are proved for the linear element in the convergence theorem. $\epsilon = 0.1$ is used to generate the table. Figure 5.3 plots the change of the discrete energy $E_h(U^\ell)$ in time, which should decrease according to (3.17). This graph clearly confirms this decay property. Figure 5.4 displays four snapshots at four fixed time points of the numerical interface with four different ϵ. They clearly indicate that at each time point the numerical interface converges to the sharp interface Γ_t of the Hele–Shaw flow as ϵ tends to zero. It again shows that the numerical interface evolves faster in time for larger ϵ and confirms the mass conservation property of the Cahn–Hilliard problem as the total mass $m = \int_\Omega u\,dx$ equals a constant value 3.032 when $\epsilon = 0.125$.

REFERENCES

[1] R. A. Adams, *Sobolev Spaces*, Academic Press, New York, 2003.
[2] N. D. Alikakos, P. W. Bates, and X. Chen, *Convergence of the Cahn-Hilliard equation to the Hele-Shaw model*, Arch. Ration. Mech. Anal., 128 (1994), pp. 165–205.
[3] A. C. Aristotelous, O. A. Karakashian, and S. M. Wise, *A mixed discontinuous Galerkin, convex splitting scheme for a modified Cahn-Hilliard equation*, Discrete Contin. Dyn. Syst. Ser. B, 18 (2013), pp. 2211–2238 .
[4] S. C. Brenner and L. R. Scott, *The Mathematical Theory of Finite Element Methods*, Springer, New York, 2008.
[5] J. W. Cahn and J. E. Hilliard, *Free energy of a nonuniform system* I*, Interfacial free energy*, J. Chem. Phys., 28 (1958), pp. 258–267.
[6] X. Chen, *Spectrum for the Allen-Cahn and Cahn-Hilliard and phase-field equations for generic interfaces*, Comm. Partial Differential Equations, 19 (1994), pp. 1371–1395.
[7] X. Chen, *Global asymptotic limit of solutions of the Cahn-Hilliard equation*, J. Differential Geom., 44 (1996), pp. 262–311.
[8] Z. Chen and H. Chen, *Pointwise error estimates of discontinuous Galerkin methods with penalty for second-order elliptic problems*, SIAM J. Numer. Anal., 42 (2004), pp. 1146–1166.
[9] Q. Du and R. A. Nicolaides, *Numerical analysis of a continuum model of phase transition*, SIAM J. Numer. Anal., 28 (1991), pp. 1310–1322.
[10] T. Dupont, *Some L^2 error estimates for parabolic Galerkin methods*, in The Mathematical Foundations of the Finite Element Method with Applications to Partial Differential Equations, Academic Press, New York, 1972, pp. 491–504.
[11] C. M. Elliott and D. A. French, *A nonconforming finite-element method for the two-dimensional Cahn-Hilliard equation*, SIAM J. Numer. Anal., 26 (1989), pp. 884–903.
[12] X. Feng, *Fully discrete finite element approximations of the Navier–Stokes–Cahn–Hilliard diffuse interface model for two phase fluid flows*, SIAM J. Numer. Anal., 44 (2006), pp. 1049–1072.
[13] X. Feng and Y. Li, *Analysis of symmetric interior penalty discontinuous Galerkin methods for the Allen-Cahn equation and the mean curvature flow*, IMA J. Numer. Anal., 35 (2015), pp. 1622–1651.
[14] X. Feng, Y. Li, and Y. Xing, *Analysis of mixed interior penalty discontinuous Galerkin methods for the Cahn-Hilliard equation and the Hele-Shaw flow*, arXiv:1502.03421, 2015.
[15] X. Feng and A. Prohl, *Error analysis of a mixed finite element method for the Cahn-Hilliard equation*, Numer. Math., 74 (2004), pp. 47–84.
[16] X. Feng and A. Prohl, *Numerical analysis of the Cahn-Hilliard equation and approximation for the Hele-Shaw problem*, Interfaces Free Bound., 7 (2005), pp. 1–28.
[17] X. Feng and H. Wu, *A posteriori error estimates and an adaptive finite element algorithm for the Cahn-Hiliard equation and the Hele-Shaw flow*, J. Comput. Math., 26 (2008), pp. 767–796.
[18] O. Karakashian and F. Pascal, *Adaptive discontinuous Galerkin approximations of second order elliptic problems*, in Proceedings of European Congress on Computational Methods in Applied Sciences and Engineering, 2004.
[19] R. L. Pego, *Front migration in the nonlinear Cahn-Hilliard equation*, Proc. Roy. Soc. London Ser. A, 422 (1989), pp. 261–278.
[20] G. B. McFadden, *Phase field models of solidification*, Contemp. Math., 295 (2002), pp. 107–145.
[21] B. Riviere, *Discontinuous Galerkin Methods for Solving Elliptic and Parabolic Equations: Theory and Implementation* Frontiers in Appl. Math., SIAM, Philadelphia, 2008.
[22] B. Stoth, *Convergence of the Cahn-Hilliard equation to the Mullins-Sekerka problem in spherical symmetry*, J. Differential Equations, 125 (1996), pp. 154–183.